

Phase transitions and their co-existence in $\text{TlGaSe}_2\text{--TlCrS}_2(\text{Se}_2)$ systems

R G VELIYEV^{a,*}, MIR HASAN YU SEYIDOV^{a,b}, E M KERIMOVA^a, R Z SADYKHOV^a,
YU G ASADOV^a, F M SEYIDOV^a and N Z GASANOV^a

^aInstitute of Physics, Azerbaijan National Academy of Sciences, Az 1143, Baku, Azerbaijan

^bDepartment of Physics, Gebze Institute of Technology, Gebze 41400, Kocaeli, Turkey

MS received 25 June 2011; revised 30 January 2012

Abstract. Investigation of dielectric properties of layered compound, TlGaSe_2 , showed that it is a ferroelectric ($T_C = 105.5$ K) with an intermediate incommensurate phase ($T_i = 114.5$ K). Our magnetic studies of layered compounds, TlCrS_2 and TlCrSe_2 , for the first time revealed that the magnetic phase transition in these compounds are quasi two-dimensional ferromagnetic in nature and magnetic characteristics are $T_C = 90$ K, $T_C^p = 115$ K, $\mu_{\text{eff}} = 3.26 \mu_B$ and $T_C = 105$ K, $T_C^p = 120$ K, $\mu_{\text{eff}} = 3.05 \mu_B$, respectively. Using the method of DTA, areas of homogeneous and heterogeneous coexistence of ferroelectric and ferromagnetic phase transitions in the systems, $\text{TlGaSe}_2\text{--TlCrS}_2$ and $\text{TlGaSe}_2\text{--TlCrSe}_2$, were identified. The low-dimensional solid solutions and eutectic alloys in these systems can be used as basic materials for plenty of functional recorders.

Keywords. Crystal growth; dielectric properties; ferroelectrics; ferromagnets; magnetic properties.

1. Introduction

Magnetolectric (ME) materials are a main class of multiferroic materials in which an applied magnetic field leads to an electric polarization response or, conversely, an applied electric field results in a magnetization response (Hill 2000; Fiebig 2005; Ma *et al* 2011). These materials have the potential for applications in modern solid-state electronics and functionalized materials, including applications in spintronics (Testino *et al* 2006; Martin *et al* 2008). Apart from potential practical applications, the fundamental physics and chemistry of ME materials are also promising. Search and preparation of ME materials could help in designing new original materials with rather unusual magnetic and dielectric properties differing from the properties of the parent phases (ferro-, antiferro-, ferri-electricity/or magnetism) and with the possibility to manipulate the magnetic properties through electric fields and *vice versa*.

Generally, because of the structural restrictions, ferroelectricity is not compatible with ferromagnetism (Martin *et al* 2008). As is known, ferroelectricity appears only in a non-centrosymmetric structure in contrast to a magnetic ion preferring a centrosymmetric surrounding. Hence, magnetolectrics are very rare materials and, until now, only a few compounds have been reported to exhibit both ferroelectric and ferromagnetic properties within the same phase. The requirements of obtaining both ferroelectric and magnetic orders in the same material can be summarized as

follows: (i) the presence of adequate structural building blocks permitting ferroelectric-type ionic movements, i.e. off-centre displacement associated with the spontaneous polarization in ferroelectrics; (ii) magnetic interaction pathways for the magnetic order, usually of the super-exchange type and (iii) symmetry conditions (Buscaglia *et al* 2006; Testino *et al* 2006).

ME materials can be either single phase or composites. There is a scarcity of homogeneous single phase bulk materials exhibiting ME behaviour (Fiebig 2005; Buscaglia *et al* 2006; Testino *et al* 2006; Martin *et al* 2008; Ma *et al* 2011). Recently, much attention has been paid to the realization of composites from heterostructural layers, piezoelectric and magnetostrictive phases, which could be electromagnetically coupled *via* stress mediation (Fiebig 2005; Buscaglia *et al* 2006; Testino *et al* 2006; Martin *et al* 2008; Ma *et al* 2011). However, structural non-compatibility and reactivity between the two materials and also with the substrate, generates immense difficulties in growing heterostructures and achieving coupling between the two coupled degrees of freedom based on local off-centred polar distortion and electron spin. Hence, the search for new chemical equilibrium homogeneous bulk magnetolectric compounds with a simple and cost-effective preparation technology is still relevant.

In the present work, the solid solutions of $\text{TlGaSe}_2\text{--TlCrS}_2$ and $\text{TlGaSe}_2\text{--TlCrSe}_2$ have been prepared with a view to obtaining co-existence of ferroelectric and ferromagnetic properties in the same compound under the same range of temperatures. We assume to combine ferroelectrics, TlGaSe_2 with magnetic materials, TlCrS_2 and TlCrSe_2 , creating solid solutions by partly substituting Cr at the Ga site without disturbing the ferroelectric properties of TlGaSe_2 .

*Author for correspondence (ramizveliyev@gmail.com)

The solid solutions, $\text{TlGaSe}_2\text{-TlCrS}_2$ and $\text{TlGaSe}_2\text{-TlCrSe}_2$, could be a new class of ME materials with effective and simple preparation technology meeting all conditions for ME specified above. In connection with the above, dielectric properties of layered compound, TlGaSe_2 and magnetic properties of layered compounds, TlCrS_2 and TlCrSe_2 , were investigated. The molar relations in the systems of $\text{TlGaSe}_2\text{-TlCrS}_2$ and $\text{TlGaSe}_2\text{-TlCrSe}_2$ were characterized by differential thermal analysis (DTA).

2. Sample preparation and experimental

2.1 Preparation of TlGaSe_2 , TlCrS_2 and TlCrSe_2 crystals

TlGaSe_2 , TlCrS_2 and TlCrSe_2 polycrystals were synthesized from extra pure (at least 99.999%) elements taken in stoichiometric proportions in vacuum-sealed ($\sim 10^{-3}$ Pa) silica tubes at a temperature of ~ 1150 K. Chromium was preliminarily powdered using a ball mill. The synthesis was conducted by an inclined furnace method for ~ 120 h. The angle of the furnace was $\sim 30^\circ$. Obtained reaction products were powdered, pressed and subjected to homogenizing annealing in evacuated sealed silica tubes at a temperature of 600 K for 480 h. TlGaSe_2 , TlCrS_2 and TlCrSe_2 samples had red, black and grey colours, respectively. The chemical compositions of the TlGaSe_2 , TlCrS_2 and TlCrSe_2 crystals were determined by using energy dispersive spectroscopic analyses with a JSM-6400 electron microscope. The energy dispersive X-ray analysis performed at room temperature confirmed the formula composition of all the samples.

2.2 Experimental procedure

For investigation of the temperature dependence of dielectric permittivity, $\varepsilon(T)$, of the layered compound, TlGaSe_2 , samples in the form of plates, cut out from the single-crystal ingot of this compound, were used. The single-crystal ingot of TlGaSe_2 was grown by Bridgman-Stockbarger method; in this case the rate of movement of crystallization front was 1 mm/h. The plates of TlGaSe_2 had ~ 2 mm thickness and ~ 20 mm² surface area and were cut parallel to [010] axis. For $\varepsilon(T)$ measurements, two gold electrodes were attached by the vacuum deposition method along the [010] axis. The distance between the electrodes was ~ 2 mm. Thin copper wires were attached to the electrodes by high-purity silver paste drops for circuit connections. The electrical conductivity of the studied sample was *p*-type. The freshly cleaved platelets (along the layer plane (001)) were mirror-like. Therefore, no further polishing and cleaning treatments were required.

The $\varepsilon(T)$ of the TlGaSe_2 crystal was measured by the automatic digital precision LCR meters at a frequency of 1 kHz. The relative error in the determination of the permittivity was less than $\sim 0.2\%$. The temperature of the sample was measured with a copper-constantan thermocouple. The

thermocouple junction was located in the vicinity of the sample surface. Temperature of the sample was controlled by a PID digital temperature controller within ± 0.01 K.

The pyroelectric properties of TlGaSe_2 were studied by quasistatic method in the short-circuit regime. The temperature was changed with the rate of ~ 20 K/min and pyroelectric current was measured using a high precision digital Keithley-485 picoammeter. The silver paste was painted onto the surfaces of the doped TlGaSe_2 sample perpendicular to the polar [010] axis to form electrodes. Two thin wire terminals were used as external leads to make the sample free and to avoid any stress on it. Prior to the measurements, sample was subjected to electrical poling by cooling in darkness from room temperature to 77 K in the presence of polarizing electric field, ~ 3 kV/cm, generated by high voltage power supply.

The temperature dependence of specific magnetization (σ_{sp}) and paramagnetic susceptibility (χ) of TlCrS_2 and TlCrSe_2 crystals were measured by a Domenicalli pendulum magnetometer and Faraday method (on magnetoelectric scales), respectively. Polycrystalline samples for the magnetic measurements had cylindrical shape with dimensions of height, ~ 3 mm and diameter, ~ 2.5 mm.

Dielectric and magnetic measurements were performed in the 77–300 K temperature range, in the quasistatic regime. The sample was mounted on the cold finger of the liquid nitrogen cryostat equipped with a temperature stabilization system with an accuracy of ± 0.05 K. The rate of temperature change was about 1 K/min.

Molar relations in the systems $\text{TlGaSe}_2\text{-TlCrS}_2$ and $\text{TlGaSe}_2\text{-TlCrSe}_2$ were investigated by DTA method. DTA was performed on low frequency thermograph recorder NTR-64 which allowed measurement of the temperature of phase transformation with an accuracy of ± 5 K. Heating rate was about 2–4 K/min. Temperature was controlled by Pt–Pt/Rh thermocouple, graded according to fiducial elements in the interval of 430–1560 K.

2.3 Detailed room temperature structural characterization

X-ray diffraction (XRD) analysis of TlGaSe_2 , TlCrS_2 and TlCrSe_2 samples, specially prepared after annealing, was performed at room temperature (~ 300 K) using DRON-3M diffractometer ($\text{CuK}\alpha$ radiation, Ni filter, $\lambda = 0.15418$ nm, 35 kV, 10 mA). Reflection coefficients were determined within an error of $\sim 0.01^\circ$. The diffraction angles were determined by measuring the maximum intensity of diffraction reflections. XRD patterns were obtained in the 2θ range varying from 10 to 70° , where errors for determination of the peak position did not exceed $\Delta\theta = \pm 0.02^\circ$.

The X-ray diffraction reflections of TlGaSe_2 and TlCrS_2 as well as TlCrSe_2 crystals are summarized in tables 1 and 2. The diffractograms of TlGaSe_2 , TlCrS_2 and TlCrSe_2 are indexed by syngonies in a monoclinic and hexagonal crystalline structure with parameters (tables 1 and 2) $a = 10.771$ Å, $b = 10.769$ Å, $c = 15.638$ Å, $\beta = 100^\circ 04'$, $z = 16$, $\rho_x = 6425$ kg/m³; $a = 3.538$ Å, $c = 21.962$ Å, $c/a = 6.207$,

$z = 3$, $\rho_x = 6705 \text{ kg/m}^3$ and $a = 3.707 \text{ \AA}$, $c = 22.688 \text{ \AA}$, $c/a = 6.120$, $z = 3$, $\rho_x = 6186 \text{ kg/m}^3$, respectively. It should be noted that our XRD data for $TlGaSe_2$ is in good agreement with single $TlGaSe_2$ crystal X-ray diffraction data reported in the literature (Muller and Hahn 1978).

In Rosenberg *et al* (1982) work, the samples of $TlCrS_2$ were prepared by passing H_2S over $Tl_2Cr_2O_7$ or $TlCrCl_4$ at a temperature of about 700 K for 12 h. The samples of $TlCrSe_2$ were prepared by heating the binary chalcogenides, Tl_2Se and Cr_2Se_3 , in an evacuated sealed silica tube at 750 K for five days. In this work (Rosenberg *et al* 1982), the crystalline structures of $TlCrS_2$ and $TlCrSe_2$ were found to be rhombohedral. It has also been reported that $TlCrS_2$ and $TlCrSe_2$ are ferromagnets.

However, in contrast to the data of Rosenberg *et al* (1982), our XRD data for samples $TlCrS_2$ and $TlCrSe_2$ cannot be

indexed in the rhombohedral crystalline structure. We carried out indexing in the hexagonal crystalline structure (see table 2).

3. Results and discussion

3.1 Ferroelectric property of $TlGaSe_2$

$TlGaSe_2$ is a ferroelectric semiconductor which crystallizes into a monoclinic structure at room temperature. The lattice of $TlGaSe_2$ consists of alternating two-dimensional layers stacked in the direction parallel to the crystallographic c -axis, with each successive layer turned at a right angle with respect to the preceding layer (Muller and Hahn 1978). The fundamental structural unit of a layer is the Ga_4Se_{10} polyhedron representing a combination of four elementary $GaSe_4$ tetrahedra linked together by bridging Se atoms. The combination of the Ga_4Se_{10} polyhedra within a layer results in trigonal prismatic voids where Tl atoms are located. Tl atoms form nearly planar chains along the $[110]$ and $[1\bar{1}0]$ directions. The number of layers within the unit cell is two (Muller and Hahn 1978).

$TlGaSe_2$ undergoes a sequence of structural phase transitions with temperature: a second order phase transition from a paraelectric phase to intermediate incommensurate (INC) phase at about $T_i \sim 120 \text{ K}$ and a first order phase transition from the INC phase to a ferroelectric phase at $T_c \sim 110 \text{ K}$ (McMoorrow *et al* 1990). The X-ray studies of $TlGaSe_2$ (McMoorrow *et al* 1990) show that the incommensurate modulation wave vector is $\vec{k} = (\delta; \delta; 0.25)$ with $\delta = 0.02$. At the T_c , lock-in transition is realized, $\delta = 0$, into commensurate (C) improper ferroelectric state with unclear space group. The lattice constant \vec{c} is quadrupled below T_c and a spontaneous polarization appears parallel to the layers plane in C-phase.

Figure 1 demonstrates a typical $\varepsilon(T)$ of $TlGaSe_2$. As it is seen from the figure, curve $\varepsilon(T)$ of $TlGaSe_2$ contains anomalies in the form of maxima, connected to the phase transition

Table 1. X-ray diffraction analysis of $TlGaSe_2$.

No.	I/I_0	$d_{\text{exp.}}$ (nm)	$d_{\text{calc.}}$ (nm)	hkl
1.	20	0.44102	0.44102	122
2.	5	0.40277	0.40272	202
3.	100	0.38430	0.38421	004
4.	20	0.35575	0.35598	221
5.	5	0.34005	0.34002	130
6.	5	0.32514	0.32560	114
7.	20	0.32054	0.32252	222
8.	70	0.28992	0.28940	312
9.	10	0.26749	0.26695	025
10.	60	0.25947	0.25947	034
11.	5	0.24001	0.24001	240
12.	5	0.21190	0.21110	150
13.	5	0.20271	0.20377	117
14.	20	0.19311	0.19270	153
15.	20	0.19143	0.19204	512
16.	5	0.18241	0.18221	154
17.	20	0.17096	0.17079	208
18.	10	0.16199	0.16204	119

Table 2. X-ray diffraction analysis of $TlCrS_2$ and $TlCrSe_2$.

$TlCrS_2$				$TlCrSe_2$				
I/I_0	$d_{\text{exp.}}$ (nm)	$d_{\text{calc.}}$ (nm)	hkl	No.	I/I_0	$d_{\text{exp.}}$ (nm)	$d_{\text{calc.}}$ (nm)	hkl
50	0.7314	0.7307	0003	1.	50	0.7565	0.7563	0003
20	0.4388	0.4384	0005	2.	10	0.4537	0.4538	0005
100	0.3662	0.3653	0006	3.	80	0.3781	0.3782	0006
70	0.3065	0.3064	10 $\bar{1}$ 0	4.	40	0.3242	0.3241	0007
10	0.3034	0.3035	10 $\bar{1}$ 4	5.	15	0.2950	0.2950	10 $\bar{1}$ 3
40	0.2688	0.2675	10 $\bar{1}$ 5	6.	10	0.2837	0.2836	0008
40	0.2513	0.2512	0009	7.	20	0.2791	0.2790	10 $\bar{1}$ 4
30	0.2443	0.2436	00010	8.	50	0.2629	0.2617	10 $\bar{1}$ 5
20	0.2201	0.2192	10 $\bar{1}$ 8	9.	100	0.2522	0.2521	0009
10	0.2043	0.2043	10 $\bar{1}$ 9	10.	20	0.1890	0.1891	00012
20	0.1913	0.1907	00012	11.	50	0.1852	0.1851	00015
25	0.1440	0.1446	20 $\bar{2}$ 5	12.	20	0.1512	0.1513	20 $\bar{2}$ 5

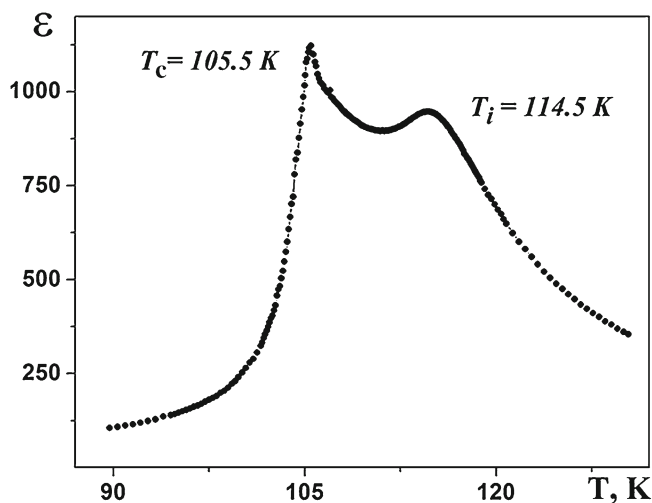


Figure 1. Temperature dependence of dielectric permittivity of TiGaSe₂.

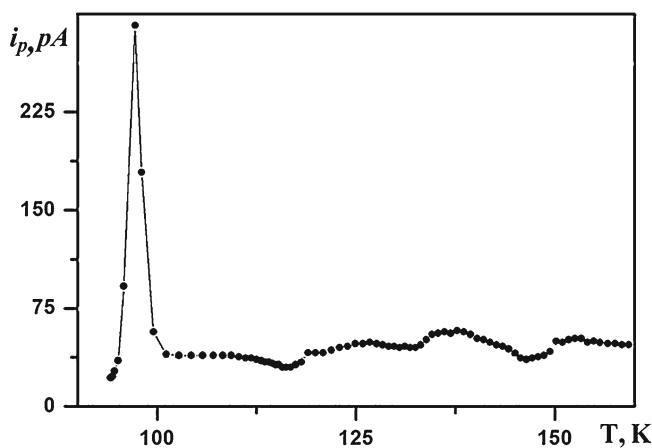


Figure 2. Temperature dependence of pyrocurrent for TiGaSe₂ when sample was cooled in presence of d.c. electric field, $E = 3$ kV/cm from 300 to 77 K.

points in the INC phase at $T_i = 114.5$ K and C-ferroelectric phase at $T_c = 105.5$ K. $\varepsilon(T)$ of TiGaSe₂ in the paraelectric and ferroelectric phases is well approximated by Curie–Weiss law with a value of Curie constant of $\sim 10^3$ K.

Figure 2 demonstrates temperature dependences of pyrocurrent, $i_p(T)$, for the same TiGaSe₂ sample. It has been found that the maximum of $i_p(T)$ in TiGaSe₂ crystal is registered at temperature ~ 97 K close to T_c (as is known, the peak of $i_p(T)$ is always recorded at temperatures lower than T_c). Thus, TiGaSe₂ samples used in this study were ferroelectrics in the temperature region, $T < T_c$.

3.2 Magnetic properties of TiCrS₂ and TiCrSe₂

Low symmetry of crystalline structure of TiMeX₂ type magnets (where Me = 3d metal; X = S, Se, Te) (Kutoglu 1974; Klepp and Boller 1979; Zabel and Range 1979; Rosenberg

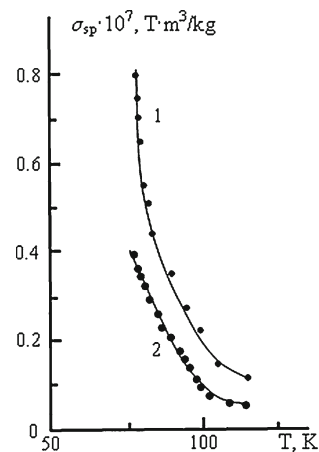


Figure 3. Temperature dependence of specific magnetization of TiCrS₂ (1) and TiCrSe₂ (2).

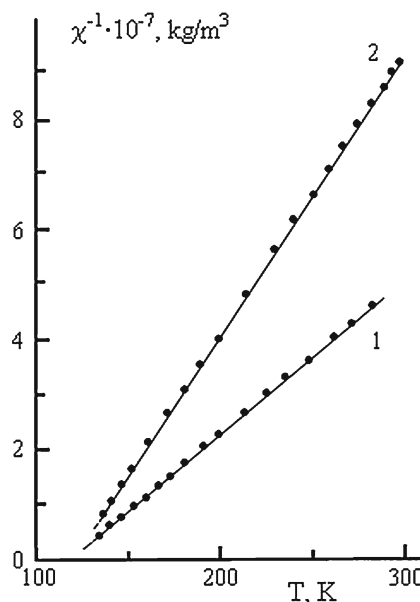


Figure 4. Temperature dependence of inverse magnetic susceptibility of TiCrS₂ (1) and TiCrSe₂ (2).

et al 1982; Makovetskiy and Kasinskiy 1984; Veliyev *et al* 2008) predefines dependence of their magnetic properties from basic crystallographic directions. In some cases (structure has plain or chain constructions)—up to the occurrence of low-dimensional effect, when spin system (magnetic structure) of the magnet in paramagnetic area, in certain temperature interval, is in quasi-two-dimensional or quasi-one-dimensional magnetic ordering (Ising–Heisenberg model) (Aleksandrov *et al* 1983). According to this model, behaviour of low-dimensional spin systems in the area of high temperatures (paramagnetic area), in the vicinity of three-dimensional magnetic phase transition and in the area of low temperatures, has specific peculiarities, which sharply differ from the behaviour of three-dimensional spin systems.

For example, temperature dependence of magnetic susceptibility of low-dimensional antiferromagnet in paramagnetic area of temperatures with $T \gg T_N$ (T_N —Neel point, which characterizes the long-range magnetic ordering), is characterized by the presence of wide maximum, which is associated with a strong short-range magnetic order. Also on the temperature dependence of thermal capacity of low-dimensional magnetic anomaly with evident deviation from λ -type is observed. This experimental fact predetermines much greater magnitude value of T_C^P than T_C (specific feature in the vicinity of three-dimensional magnetic phase transition). For three-dimensional isotropic magnets, difference between the temperatures that characterize the long-range and short-range magnetic order is small and amounts to 3–5% of the temperature, which characterizes short-range magnetic order (Aleksandrov *et al* 1983).

Figure 3 shows temperature dependence of specific magnetization of $TlCrS_2$ and $TlCrSe_2$, measured by us in a magnetic field of 8×10^5 A/m. As can be seen from figure 3, values of the magnetization of $TlCrS_2$ and $TlCrSe_2$, in contrast to the values reported by Rosenberg *et al* (1982), are small and at a temperature of about 100 K for both compounds and their rapid growth is observed. Treatment of the

experimental results in the area of magnetic transformation by the method of thermodynamic coefficients (Belov and Goryaga 1956) showed that the Curie temperature of $TlCrS_2$ is 90 K and $TlCrSe_2$ is 105 K.

Figure 4 shows temperature dependence of inverse magnetic susceptibility, $\chi^{-1}(T)$, of the compounds $TlCrS_2$ and $TlCrSe_2$, which indicates that there are ferromagnets. Paramagnetic Curie temperature determined by extrapolating $\chi^{-1}(T)$ to the temperature axis, is equal to 115 K and 120 K for $TlCrS_2$ and $TlCrSe_2$, respectively. In contrast to Rosenberg *et al* (1982), in our case T_C^P for both compounds is significantly larger than T_C . This fact corresponds to the Ising–Heisenberg model in the vicinity of three-dimensional magnetic phase transition (Aleksandrov *et al* 1983).

The effective magnetic moment (μ_{eff}) was calculated from the dependence of $\chi^{-1}(T)$ and is equal to $3.26 \mu_B$ for $TlCrS_2$ and $3.05 \mu_B$ for $TlCrSe_2$. The theoretical value, which is calculated taking into account the value of spin magnetic moment of the Cr^{3+} ion, is $3.85 \mu_B$. The rather larger deviation of μ_{eff} from the theoretical value indicates the presence of quasi two-dimensional magnetic ordering in the paramagnetic area of layered ferromagnets, $TlCrS_2$ and $TlCrSe_2$. Low-dimensional magnetic structure of these ferromagnets is also noted in Aldzhanov *et al* (1996, 2007).

The distinction of magnetic characteristics (T_C , T_C^P , μ_{eff}) of the ferromagnets of $TlCrS_2$ and $TlCrSe_2$ are determined

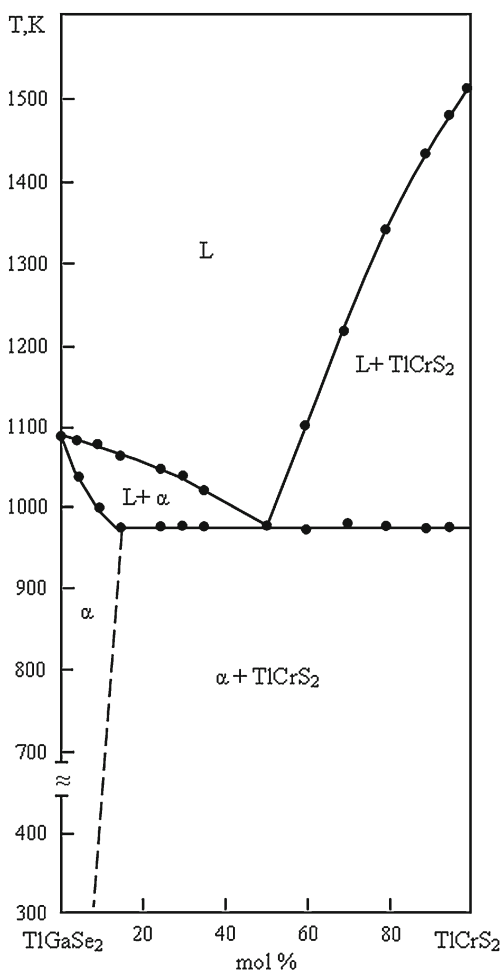


Figure 5. Schematic diagram of $TlGaSe_2$ – $TlCrS_2$ system.

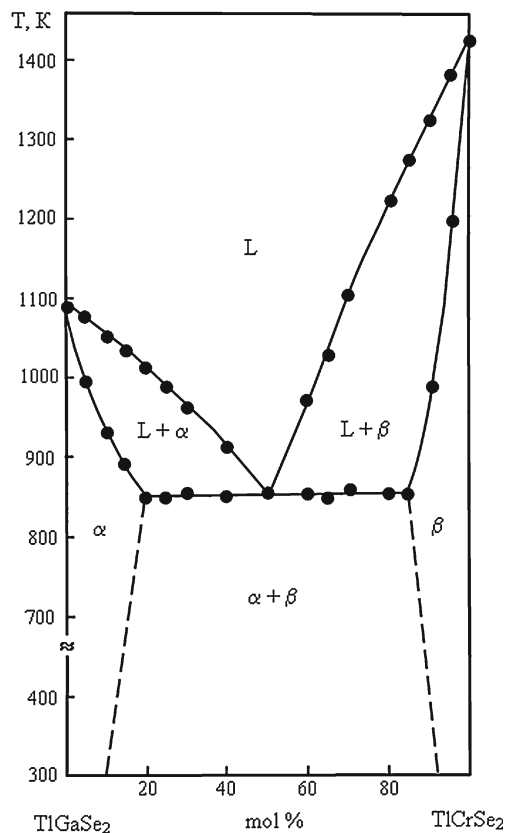


Figure 6. Schematic diagram of $TlGaSe_2$ – $TlCrSe_2$ system.

in Rosenberg *et al* (1982) is compared with our investigations which is associated with a different duration of annealing viz. 480 h, by our technology and 0 h in Rosenberg *et al* (1982). The prolonged homogenizing annealing introduces rather substantial corrections to the formation of the spin system of magnetic crystals with a complex chemical composition.

In order to solve the physical task presented in this article, it is necessary to determine areas of the homogeneous and heterogeneous co-existence of the ferroelectric TiGaSe₂ with ferromagnets TiCrS₂ and TiCrSe₂.

State diagram of TiGaSe₂–TiCrS₂ system constructed on the results of DTA is presented in figure 5. This system is eutectic type quasi-binary with solid solutions on the base of TiGaSe₂ (homogeneous area of the co-existence of ferroelectric and ferromagnetic orderings), reaching 8 mol% TiCrS₂ at a temperature of 300 K. The eutectic is formed at components ratio of 1:1. The eutectic melts at a temperature of 975 K and has the composition (TiGaSe₂)_{0.5}(TiCrS₂)_{0.5}, i.e. in this eutectic alloy ferroelectric and ferromagnetic orderings heterogeneously (compositionally) co-exist.

In figure 6, schematic diagram of TiGaSe₂–TiCrSe₂ system, also constructed on the results of DTA, is presented. This system is eutectic type quasi-binary with limited areas of solid solutions on the base of TiGaSe₂, reaching 10 mol% TiCrSe₂, and reaching 8 mol% TiGaSe₂ on the base of TiCrSe₂ (homogeneous areas of the co-existence of ferroelectric and ferromagnetic orderings) at 300 K. The eutectic forms at components ratio of 1:1. The eutectic melts at a temperature of 850 K and has the composition (TiGaSe₂)_{0.5}(TiCrSe₂)_{0.5}, i.e. in this eutectic alloy ferroelectric and ferromagnetic orderings heterogeneously (compositionally) co-exist.

4. Conclusions

Temperature dependence of the dielectric permittivity of the layered compound TiGaSe₂ has two anomalies that are associated with phase transitions in the incommensurate phase at $T_i = 114.5$ K and the commensurate ferroelectric phase at $T_c = 105.5$ K. In the paraelectric and ferroelectric phases, $\varepsilon(T)$ of TiGaSe₂ follows the Curie–Weiss law with Curie constant of about 10^3 K. Temperature dependence of pyrocurrent in TiGaSe₂ single crystal has a sharp maximum at a temperature ~ 97 K, close to T_c . Our magnetic studies of

layered compounds, TiCrS₂ and TiCrSe₂, allowed for the first time reveal that the nature of the magnetic phase transition in these compounds is quasi two-dimensional ferromagnetic. Their magnetic characteristics were found to be $T_C = 90$ K, $T_C^p = 115$ K, $\mu_{\text{eff}} = 3.26 \mu_B$ and $T_C = 105$ K, $T_C^p = 120$ K, $\mu_{\text{eff}} = 3.05 \mu_B$, respectively. By DTA method, areas of homogeneous and heterogeneous co-existence of ferroelectric and ferromagnetic orderings in the systems, TiGaSe₂–TiCrS₂ and TiGaSe₂–TiCrSe₂ were identified. The low-dimensional solid solutions and eutectic alloys of TiGaSe₂–TiCrS₂(Se₂) systems can be used as basic materials for plenty of functional recordings.

References

- Aldzhanov M, Nadzhafzade M, Seidov Z and Gasumov M 1996 *Tr. J. Phys.* **20** 1071
- Aldzhanov M A, Abdurragimov A A, Sultanova S G and Nadzhafzade M D 2007 *Phys. Solid State* **49** 309 (in Russian)
- Aleksandrov K S, Fedoseyeva N V and Spevakova I P 1983 *Magnetic phase transitions in galoid crystals* (Novosibirsk: Science) pp. 40–85 (in Russian)
- Belov K P and Goryaga A N 1956 *Fiz. Met. Metalloved.* **2** 441 (in Russian)
- Buscaglia M T, Mitoseriu L, Buscaglia V, Pallecchi I, Viviani M, Nanni P and Siri A S 2006 *J. Eur. Ceram. Soc.* **26** 3027
- Fiebig M (2005) *J. Phys. D: Appl. Phys.* **38** R123
- Hill N A 2000 *J. Phys. Chem.* **B104** 6694
- Klepp K and Boller H 1979 *Z. Monatsh. Chem.* **110** 1045
- Kutoglu A 1974 *Z. Naturwissen.* **B61** 125
- Ma J, Hu J, Li Z and Nan C-W 2011 *Adv. Mater.* **23** 1062
- Makovetskiy G I and Kasinskiy E I 1984 *Inorgan. Mater.* **20** 1752 (in Russian)
- Martin L W, Crane S P, Chu Y-H, Holcomb M B, Gajek M, Huijben M, Yang C-H, Balke N and Ramesh R 2008 *J. Phys.: Condens. Matter* **20** 434220
- McMorrow D F, Cowley R A, Hatton P D and Banyas J 1990 *J. Phys.: Condens. Matter* **2** 3699
- Müller D and Hahn H 1978 *Z. Anorg. Allg. Chem.* **438** 258
- Rosenberg M, Knulle A, Sabrowsky H and Platte C 1982 *J. Phys. Chem. Solids* **43** 87
- Testino A, Mitoseriu L, Buscaglia V, Buscaglia M T, Pallecchi I, Albuquerque A S, Calzona V, Marre D, Siri A S and Nanni P 2006 *J. Eur. Ceram. Soc.* **26** 3031
- Veliyev R G, Sadykhov R Z, Asadov Yu G, Kerimova E M and Jabbarov A I 2008 *Crystallogr. Rep.* **53** 130
- Zabel M and Range K 1979 *Z. Naturforsch.* **B34** 1